Joanna KOLAŃSKA-PŁUSKA[1], Jerzy BARGLIK[2], Bernard BARON[3] , Zygmunt PIĄTEK[4],

Opole University of Technology Faculty of Electrical Engineering, Automatic Control and Informatics (1)
Silesian University of Technology Faculty of Materials Sciences and Metallurgy (2)
Silesian University of Technology Faculty of Electrical Engineering (3)
Czestochowa University of Technology Faculty of Environmental Engineering and Protection (4)

The magnetic field of the tubular rectangular high current busduct of finite length

***Abstract**. The paper encloses the results of rectangle wires phenomena computation. The simulation was analyzed in the Femm 4.2. program. Numerical simulation was made for frequency 9835 Hz. The calculations of the electromagnetic field was made with the finite element method shows that FEMM software is useful tool for the initial analysis for electromagnetic field in the induction heaters. It can be successfully used for the calculation of approximate self-impedance values of rectangular cross section wires inclusive skin effect and proximity phenomenon.*

Streszczenie.** W pracy przedstawiono rozkład pola magnetycznego w przewodach szynowych o profilu prostokątnym wiodących prąd sinusoidalnie zmienny, służących do zasilania wzbudnika wewnętrznego układu nagrzewnicy indukcyjnej. Wykonano wielowariantową symulację komputerową w programie FEMM ver. 4.2. Wyznaczono rozkłady gęstości prądu i pola magnetycznego przewodach szynowych o profilu prostokątnym. Analizę przeprowadzono dla częstotliwości 9835 Hz. Uwzględniono zjawisko naskórkowości oraz efekt zbliżenia.**(Pole magnetyczne rurowego prostokątnego toru wielkoprądowego o skończonej długości)

Słowa kluczowe: Pole elektromagnetyczne, nagrzewanie indukcyjne, hartowanie indukcyjne, naskórkowość.
Keywords: Electromagnetic field, induction heating, induction hardening, skin effect.

Introduction

In the process of induction heating of metals often inductor is powered by a single phase transmission line formed on the tubular rails with rectangular profile [1-7]. This allows simultaneous cooling of the track with water flowing inside the phase conductors. One example of the Induction heating systems of the internal coil in the induction hardened pipe loads [8-11] is the system shown in Figures 1 and 2. It uses busburs rectangular pipe.

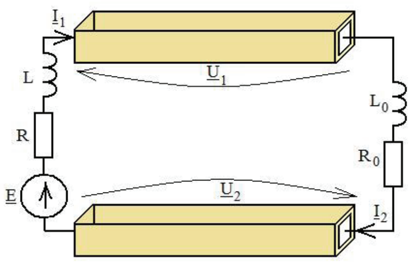

Fig.1. Induction heating diagram: $\underline{E}$, R, L - power source inside parameters, R_0, L_0- workpiece and inductor parameters.

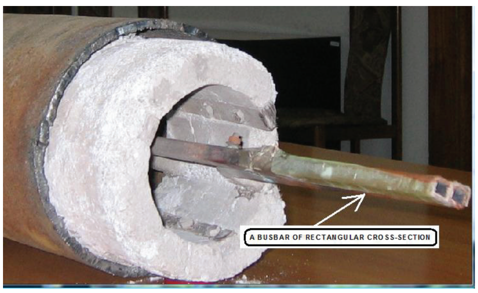

Fig. 2. A fragment of the real cross-section showing subway

In the study of the electromagnetic field of such a system should take into account the phenomenon of skin effect and the approximate due to the medium and high frequency current used in the process of heating. These phenomena give rise to uneven distribution of current density and magnetic field in busbars, which in turn significantly influence the size of losses in the track, the temperature distribution, electrodynamic force between the wires and the replacement of the transmission line parameters [6, 12-20].

The distribution of the electromagnetic field in the vicinity of the high current busducts without regard and taking into account skin effect and proximity effects, and its electrical parameters was determined in a number of works by analytical methods, numerical and analytical-numerical characters used for the rectangular busbars in power [19, 21-27].

However, in the work of these and other busducts shall be extended, allowing you consider the electromagnetic field 2-D system. In the works [28-32] was determined distributions of the magnetic field of a single wire track of solid rectangular finite length, but, assuming even distribution of power.

This article attempts to develop algorithms and methods for determining the electromagnetic field in a single phase circuit of such busbars of finite length, taking into account skin effect and proximity effects. System implemented in the program FEMM ver. 4.2.

Construction of mathematical model

The magnetic field is time-varying, eddy currents can be induced in materials with a non-zero conductivity. Several other Maxwell's equations related to the electric field distribution must also be accommodated. Denoting the electric field intensity as ***E*** and the current density as ***J*** obey the constitutive relationship:

$$\boldsymbol{J} = \sigma \boldsymbol{E} \tag{1}$$

We use also the Maxwell's equations:

$$\nabla \times \boldsymbol{H} = \boldsymbol{J} + \frac{\partial \boldsymbol{D}}{\partial t} \tag{2}$$

$$\nabla \times \boldsymbol{E} = -\frac{\partial \boldsymbol{B}}{\partial t} \tag{3}$$

$$\nabla \cdot \boldsymbol{B} = 0 \tag{4}$$

$$\nabla \cdot \boldsymbol{D} = \rho \tag{5}$$

Then we take a system of two straight wires of length L and rectangular cross section with sides b, h, l the thickness, electrical conductivity σ, made of material with a permeability μ_o non ferromagnetic (Fig. 3).

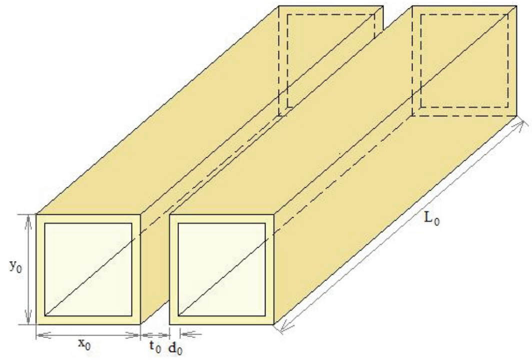

Fig.3. A busbar of pipes rectangular cross-section

Let between the ends of these wires are forced sinusoidally time-varying potential differences in the pulsation ω whose values are complex, $\underline{U}_1$ and $\underline{U}_2$ (Fig. 1). Forced in this way the electric field inside the pipe $-\mathbf{grad}\underline{V}(X)$ causes the rate of flow of a current density of the complex $\underline{\boldsymbol{J}}(X)$, which in turn induces the wires inside and outside the complex electric field induction equal $-\mathrm{j}\omega\underline{\boldsymbol{A}}(X)$. Accident complex electric field then takes the form [34]:

$$\underline{\boldsymbol{E}}(X) = -\mathbf{grad}\,\underline{V}(X) - \mathrm{j}\omega\underline{\boldsymbol{A}}(X) \tag{6}$$

where the composite magnetic vector potential

$$\underline{\boldsymbol{A}}(x_1,x_2,x_3) = \frac{\mu_o}{2\pi}\cdot \sum_{p=1}^{2}\int_{v^{(p)}} \frac{\underline{\boldsymbol{J}}(y_1,y_2,y_3)}{\sqrt{(x_1-y_1)^2+(x_2-y_2)^2+(x_3-y_3)^2}}\mathrm{d}y_1\mathrm{d}y_2\mathrm{d}y_3 \tag{7}$$

$v^{(p)}$ - is an area in which the p-th conductor.
Taking into account Ohm's law

$$\underline{\boldsymbol{J}}(x_1,x_2,x_3) = \sigma\underline{\boldsymbol{E}}(x_1,x_2,x_3) \tag{8}$$

and equation (7) and (8), obtained by the equation

$$-\mathbf{grad}\,\underline{V}(x_1,x_2,x_3) = \frac{1}{\sigma}\underline{\boldsymbol{J}}(x_1,x_2,x_3) + \mathrm{j}\frac{\omega\mu_o}{2\pi}\cdot \sum_{p=1}^{2}\int_{v^{(p)}} \frac{\underline{\boldsymbol{J}}(y_1,y_2,y_3)}{\sqrt{(x_1-y_1)^2+(x_2-y_2)^2+(x_3-y_3)^2}}\mathrm{d}y_1\mathrm{d}y_2\mathrm{d}y_3 \tag{9}$$

The point $X(x_1,x_2,x_3)$ we determine the magnetic field strength formula

$$\underline{\boldsymbol{H}} = \frac{1}{\mu_0}\mathbf{rot}\underline{\boldsymbol{A}} = \frac{1}{\mu_0}\mathbf{rot}\underline{A}\,\mathbf{1}_z = \underline{H}_x\,\mathbf{1}_x + \underline{H}_y\,\mathbf{1}_y \tag{10}$$

where $\mathbf{1}_x$, $\mathbf{1}_y$ and $\mathbf{1}_z$ are unit vectors of Cartesian coordinates.

Module of the total magnetic field has the form

$$H(x_1,x_2,x_3) = \sqrt{H_x^2(x_1,x_2,x_3) + H_y^2(x_1,x_2,x_3)} \tag{11}$$

This module can be expressed in relative units, ie in the form

$$h(x_1,x_2,x_3) = \frac{H(x_1,x_2,x_3)}{H_0} \tag{12}$$

where volume $H_0 = \dfrac{I}{2\,(h+b)}$.

Example number

As marked on Figure 3, the following dimensions of rectangular wires: x_0=20 mm, y_0=25 mm, wall thickness of the rectangular profile t_0=2mm, profile length L = 2m. The distance between conductors is d_0=3 mm. Supply voltage frequency is 9835 Hz. Assumed that the cable is made of copper with a relative permeability μ_r=1 , and conductivity of σ=5,6·10^7 S/m . Inductor current is supplied with a value of effective 2kA. Numerical model of the high current busducts analyzed with a grid Figure 4 illustrates. For the discretization using triangular elements with linear approximation. The grid was generated independently for the busway and the surrounding airspace and consisted of 48.361 nodes and 96.686 elements.

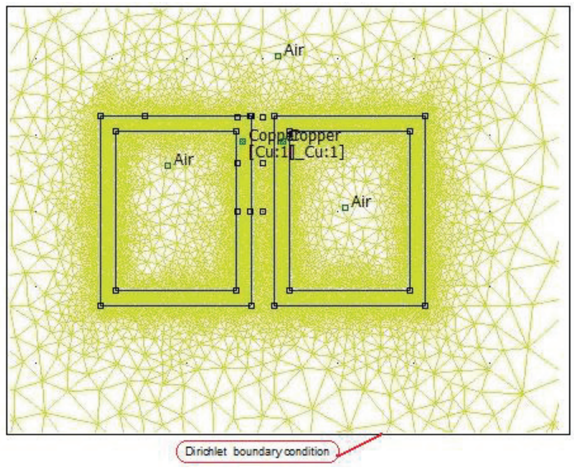

Fig. 4. Two-dimensional model of wire track with a visible grid

In such an approach is preserved continuity of the network. On the boundary of the defined boundary conditions Mixed type. This denotes a boundary condition of the form:

$$\varepsilon_r\varepsilon_0\frac{\partial A}{\partial n} + c_0A + c_1 = 0 \text{, where } c_0 = 0,\ c_1 = 0. \tag{13}$$

By the choice of coefficients, this boundary condition can either be a Robin or a Neumann boundary condition.

The Robin boundary condition is sort of a mix between Dirichlet and Neumann, prescribing a relationship between the value of *A* and its normal derivative at the boundary. An example of this boundary condition is:
$\dfrac{\partial A}{\partial n} + cA = 0$. The Dirichlet boundary condition - the value of potential *A* or *V* is explicitly defined on the boundary, *e.g.* *A* = 0. The most common use of Dirichlet-type boundary conditions in magnetic problems is to define *A* = 0 along a boundary to keep magnetic flux from crossing the boundary.

The Neumann boundary condition specifies the normal derivative of potential along the boundary. In magnetic problems, the homogeneous Neumann boundary condition,

$\frac{\partial A}{\partial n} = 0$ is defined along a boundary to force flux to pass the boundary at exactly a 90 angle to the boundary [35].

The results of calculations

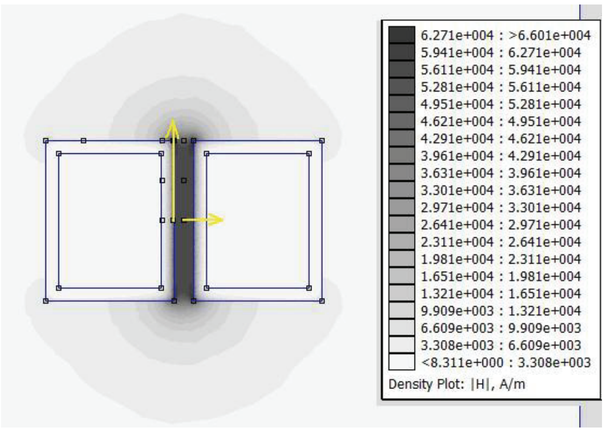

Fig. 5. Magnetic field intensity with market two straight lines. Along this lines is appointed distributions of field intensity.

Figure 6-7 present the magnetic field along the line

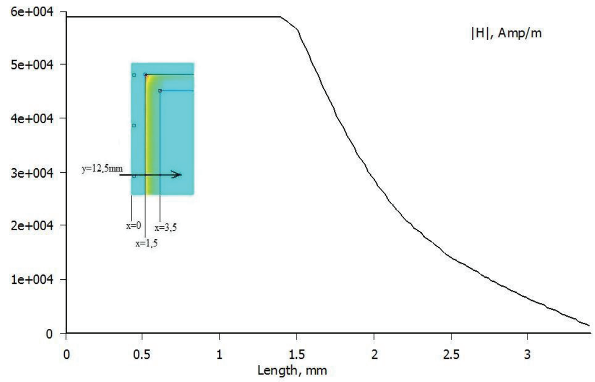

Fig. 6. Magnitude of magnetic field intensity

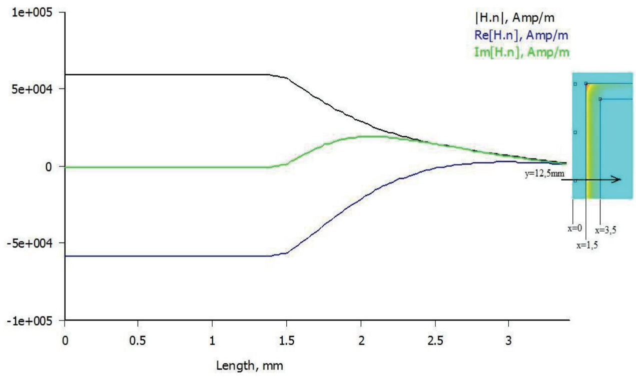

Fig. 7. Normal magnetic field intensity

Fig. 8-10 shows distributions of magnetic field intensity along the line vertical.

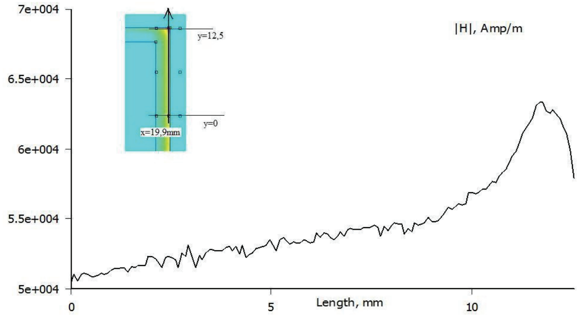

Fig. 8. Magnitude of magnetic field intensity

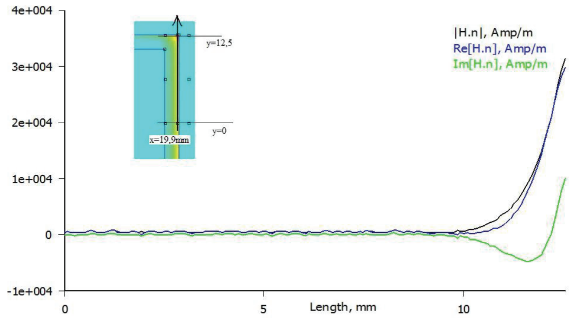

Fig. 9. Normal magnetic field intensity

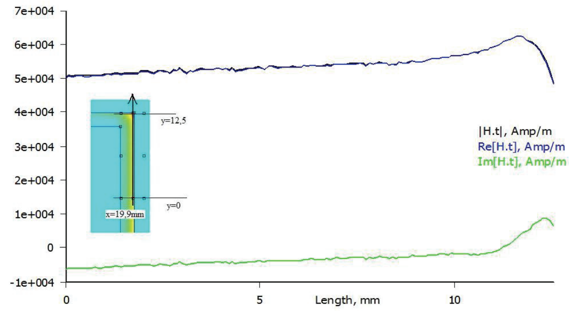

Fig. 10. Tangential magnetic field intensity

Fig. 11 shows distributions of magnetic field intensity.

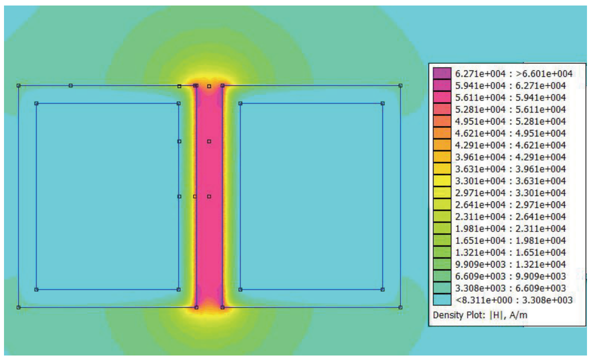

Fig.11. Magnetic field intensity

Conclusions

Using FEMM computer simulation was carried out multi-variant. In this paper we present only the results obtained for the frequency of the power source of 9835 Hz. The analysis shows that for high frequencies above 5kHz inductor current, the conductor made of copper pipe cross-section of magnetic field strength is greatest in thin wires, and then rapidly disappears. Large values of the field strength are also present in the inner corners of the wires. The highest values of magnetic field strength equal to 62.71 kA/m was obtained for the space between the two rails leading current in the opposite direction to the frequency of 9835 Hz.

This work was partly financed by the Polish Ministry of Science and Higher Education from means of budget on science in years 2010-2012 as research project N N510 256338.

REFERENCES

[1] Hering M.: *Podstawy elektrotermii. Część II.* WNT, Warszawa 1998.

[2] Langer E.: *Teorie indukčniho a dielektrickeho tepla*. Academia, Praha 1979.

[3] Davies E.J.: *Conduction and Induction Heating*. Peter Peregrinus Ltd., London 1990.

[4] Sajdak C., Semek E.: *Nagrzewanie indukcyjne. Podstawy teoretyczne i zastosowania*. Wyd. Śląsk, Katowice 1987.

[5] Barglik J., Muszyński J.: *Stanowisko do hartowania indukcyjnego rur wzbudnikiem wewnętrznym*. Materiały konferencji „Badania naukowe w elektrotermii". Wisła 1988 r. ss. 12-19.

[6] Rudnew V., Loveless D., Cook R., Black M.: *Handbook of Induction Heating*. Copyright by Marcel Dekker, New York 2003

[7] Barglik J., Doležel I., Karban P., Kwiecień I., Ulrych B.: *Comparison of two ways of induction hardening of long steel tubes*. Proceedings of the XIII International Symposium on Theoretical Electrical Engineering. ISTET'05 Lvov 2005 pp. 11-14.

[8] Piątek Z., Doležel I., Baron B.: *Pole magnetyczne we wsadzie rurowym nagrzewanym indukcyjnie od wewnątrz*. Przegląd Elektrotechniczny, Rok LXXXI, No. 6, 2005, ss. 48-51.

[9] Baron B., Kolańska-Płuska J., Krych J.: *Application of Bessel functions and discrete Fourier transform to the analysis of electromagnetic system compromised from tubular work - piece heated by induction.* XXXI IC SPETO*,* Gliwice 2008, pp. 27-28.

[10] Piątek Z., Szczegielniak T.: *Analiza numeryczna pola magnetycznego we wsadzie rurowym nagrzewanym indukcyjnie od wewnątrz*. Przegląd Elektrotechniczny, R.85, Nr 3/2009, ss. 63-66.

[11] Kolańska-Płuska J.: *The Application of FEMM Program for Numerical Analysis of Electromagnetic Field of Rectangle Wires Section in Long Iron Pipes Heardening Process*. XXXII IC SPETO*,* Gliwice 2009, pp. 31-32.

[12] Kurbiel A., Waradzyn Z.: *A method for Determining Electrical Quantities in a Workpiece Heated by Induction*. Electrical Power Quality and Utilisation, Vol. IX, No 1/2003, pp. 103-108.

[13] Chiampi M., Chiarabaglio D., Tartaglia M.: *A general approach for analyzing power busbar under AC conditions*. IEEE Trans. on Magn., Vol. 29, No. 6, November 1993, pp. 2473-2475.

[15] Du J., Burnett J., Fu Z. C.: *Experimental and numerical evaluation of busbar trunking impedance*. Electric Power Systems Research 55 (2000), pp. 113-119.

[16] Cher R., Bryant J.: *The inductance of busbars of rectangular cross-section*. Austrialian Postmaster-General's Department: Research Laboratory Report No. 4139, February 1956.

[17] Kalantarov P. L., Ciejtlin L. A.: *Calculating of inductances* (in Russian). Energija, Saint Petersburg 1970.

[18] Strunskij B. M.: *Short electric network of electric furnaces* (in Russian). GN-TIL po Cz. i CM, Moskow 1962.

[19] Au A., Maksymiuk J., Pochanke Z.: *Podstawy obliczeń aparatów elektroenergetycznych*. WNT, Warszawa 1982.

[20] Grover F. W.: *Inductance Calculations*. Dover Phoenix Editions, New York 2004.

[21] Battauscio O., Chiampi M., Chiarabaglio D.: *Experimental validation of a numerical model of busbar systems*. IEE Proc. Gener. Transm. Distrib., Vol. 142, No. 1, January 1995, pp. 65-72.

[22] Dawson F. P., Cao M., Jain P. K.: *A simplified approach to calculating current distribution in paralleled busses*. IEEE Trans. on Magn., Vol. 26, No. 2, March 1990, pp. 971-974.

[23] Kazakov M. K.: *Using the full current law in discrete form for measuring high direct currents*. Electrical technology, No. 3, 1997, pp. 143-157.

[24] Hwang C. C., Chang J. J., Jiang Y. H.: *Analysis of electromagnetic and thermal fields for a bus duct system*. Electric Power Systems Research 45 (1998), pp. 39-45.

[25] Tozoni O. W., Kolerowa T. Ja.: *Multiphase industrial busducts*. Naukowa Dumka, Kiev 1966.

[26] Du Y., Burnett J., Fu Z. C.: *Experimental and Numerical Evaluation of Busbar Trunking Impedance*. Electric Power Systems Research, No 55, 2000, pp. 113-119.

[27] Lipiński W.: *Analiza rozkładu gęstosci prądu w wydłuzonej szynie prostokątnej*. Archiwum Elektrotechniki, tom XXIII, z. 1, 1974, ss. 49-57.

[28] Piątek Z.: *Indukcyjność przewodu o przekroju prostokątnym i dowolnej długości*. Przegląd Elektrotechniczny, ISSN 0033-2097, R. 83, NR 2/2007, ss. 119-122.

[29] Piątek Z.: *Zastosowanie równania całkowego do wyznaczania impedancji własnej przewodu szynowego dowolnej długości o przekroju prostokątnym*. X Konferencja "Zastosowania komputerów w elektrotechnice" ZKwE 2006, Poznań, 18-20.04.2006, ss. 81-82.

[30] Piątek Z., Kusiak D.: *The magnetic field intensity in a busbar of a rectangular cross-section with a finite length*. XXX International Conference on Fundamentals of Electrotechnics and Circuit Theory (XXX IC SPETO'2007), Gliwice – Ustroń, pp. 249-250.

[31] Piątek Z., Kusiak D.: *The busbar of a rectangular cross-section - the magnetic field*. International Conference on Advance Methods in the Theory of Electrical Engineering Applied to Power Systems AMTEE'07, September 10-14 2007, Pilsen, Czech Republic, pp. I.23-I.24.

[32] Piątek Z., Kusiak D.: *Application of an integral equation for calculation of the impedance of any length busbar of rectangular cross-section*. ALWERS, ISBN 13: 978-83-923978-2-3, Poznań 2006, pp. 236-242.

[33] Baron B., Kolańska-Płuska J.: *Application of Bessel functions and discrete Fourier transform to the analysis of electromagnetic system comprised of conducting solid or annular cylinder and coil wound it.* Prace Naukowe Politechniki Śląskiej, Seria Elektryka Nr 2(206) Politechnika Śląska, Gliwice 2008, pp. 33-52.

[34] Krakowski M.: *Elektrotechnika teoretyczna. Pole Elektromagnetyczne*. WN PWN, Warszawa 1995.

[35] FEMM documentations: Finite Element Method Magnetics Version 4.2 User's Manual, David Meeker dmeeker@ieee.org, 2008

Auhors: dr inż. Joanna Kolańska-Płuska: Politechnika Opolska, Wydział Elektrotechniki Automatyki i Informatyki, Instytut Układów Elektromechanicznych i Elektroniki Przemysłowej, 45-036 Opole, ul. Luboszycka 7, E-mail: j.kolanska-pluska@po.opole.pl;

prof. nadzw. dr hab. Inż. Jerzy Barglik: Politechnika Śląska, Wydział Inżynierii Materiałowej i Metalurgii, Katedra Zarządzania i Informatyki, ul. Krasińskiego 8, 40-019 Katowice, E-mail: jerzy.barglik@polsl.pl;

prof. dr hab. Inż. Bernard Baron: Politechnika Śląska, Wydział Elektryczny, Instytut Elektrotechniki Teoretycznej i Przemysłowej, Zakład Teorii Elektrotechniki, ul. Akademicka 10, 44-101 Gliwice, E-mail: bernard.baron@polsl.pl;

prof. dr hab. inż. Zygmunt Piątek: Politechnika Częstochowska, Wydział Inżynierii i Ochrony Środowiska, Instytut Inżynierii Środowiska, ul. Brzeźnicka 60a, 42-200 Częstochowa, E-mail: zygmunt.piatek@interia.pl .